







Submitted: April 5, 2024

Revised: June 4, 2024

Accepted: July 30, 2024

# Influence of aluminum shell on the process of devitrification of amorphous titanium nanoparticles: molecular dynamics simulation

G.M. Poletaev<sup>1,2</sup> , Y.Y. Gafner<sup>2</sup> , S.L. Gafner<sup>2</sup> , I.V. Zorya<sup>3</sup> ,  
Y.V. Bebikhov<sup>4</sup> , A.S. Semenov<sup>4</sup> 

<sup>1</sup>Khakass State University, Abakan, Russia

<sup>2</sup>Polzunov Altai State Technical University, Barnaul, Russia

<sup>3</sup>Siberian State Industrial University, Novokuznetsk, Russia

<sup>4</sup>Polytechnic Institute of North-Eastern Federal University, Mirny, Russia

✉ gmpoletaev@mail.ru

## ABSTRACT

A study of the amorphous nanoparticle devitrification process of titanium during heating at a rate of  $5 \cdot 10^{11}$  K/s in vacuum conditions and with the presence of aluminum shell was conducted using molecular dynamics modeling. It was shown that the presence of an aluminum shell leads to a significant increase in the nanoparticle devitrification temperature of titanium. For the considered particle sizes (with diameter from 1.75 to 11 nm) the difference was approximately 200 K. In addition, it was discovered that in vacuum conditions, crystalline embryos are primarily formed near the surface of the particle, while in the presence of an aluminum shell, they are formed, on the contrary, first in the volume of the particle. Thus, according to the results of molecular dynamics modeling, a decrease in the size of titanium particles and the presence of an aluminum shell increase the temperature range for the existence of the amorphous phase of titanium.

## KEYWORDS

molecular dynamics • nanoparticle • devitrification • crystallization • amorphous metal

**Acknowledgements.** The study was funded by the Russian Science Foundation (project No. 23-12-20003, <https://rscf.ru/project/23-12-20003/>) with parity financial support from the Government of the Republic of Khakassia.

**Citation:** Poletaev GM, Gafner YY, Gafner SL, Zorya IV, Bebikhov YV, Semenov AS. Influence of aluminum shell on the process of devitrification of amorphous titanium nanoparticles: molecular dynamics simulation. *Materials Physics and Mechanics*. 2024;52(3): 86–95. [http://dx.doi.org/10.18149/MPM.5232024\\_9](http://dx.doi.org/10.18149/MPM.5232024_9)

## Introduction

In the last few decades, metallic nanoparticles have garnered substantial interest due to their distinctive physical, chemical, and optical attributes, which stem from a high percentage of free surface as well as quantum-mechanical and topological effects [1]. Besides crystalline metallic nanoparticles, there is currently a surge in interest for particles with an amorphous structure [2–5]. Amorphous particles contain atoms that are in a non-equilibrium state and possess a greater Gibbs free energy compared to atoms in a crystal. These particles exhibit a unique electronic structure, which makes them a promising candidate, particularly in the field of catalysis [6–8]. Furthermore, amorphous metals, also known as metallic glasses, boast an unusual combination of magnetic and mechanical properties, characterized by high strength, plasticity, and toughness [9,10].

In the exploration of techniques for creating and manipulating metallic nanoparticles, significant emphasis is placed on regulating the phase state, dimensions, and morphology of the particles, as these factors play a crucial role in determining their beneficial characteristics [11–14]. Consequently, investigations into the stability of phase states, the mechanisms governing phase transitions in nanoparticles, and the variables impacting the kinetics of these transitions and the temperature at which they occur are gaining heightened significance.

Presently, it is established that the melting temperature of nanoparticles tends to decrease as their size diminishes, a phenomenon attributed to the increasing ratio of surface area to volume. This trend has been substantiated through experimental studies [15–17] and computer modeling [18–21]. Additionally, computer simulations have demonstrated that the crystallization temperature during cooling from the melt is contingent upon the size and shape of the particles, which is directly related to the ratio of surface area to volume. This temperature decreases as the proportion of surface area to volume increases [19–22].

Furthermore, the mechanism and kinetics of the devitrification process in nanoparticles, which involves the loss of their amorphous state due to crystallization during heating, remain largely unexplored. The objective of this research is to investigate the devitrification process of amorphous titanium nanoparticles at the atomic level, utilizing molecular dynamics modeling in both vacuum conditions and within an aluminum shell. The additional consideration of the influence of the aluminum shell is related to the solution of the problem of reducing the temperature of initiation of the high-temperature synthesis reaction in the Ti-Al system in mixtures subjected to preliminary mechanochemical activation [23–25]. During mechanochemical activation, so-called mechanocomposites are formed, which represent a matrix of a more plastic component (in this case aluminum), in which nanoscale particles of a more brittle component of the mixture (titanium) are located [24,25]. Such a system is characterized by a high degree of non-equilibrium due to a high concentration of defects and even the presence of an amorphous phase, which is formed as a result of intense deformation. It is noted that the beginning of the burning reaction in such a non-equilibrium system begins at temperatures significantly lower than the melting temperature of aluminum [24,25].

One of the advantages of computer modeling is the ability to study the influence of one of the factors (presence of high density of grain boundaries, dislocations, internal stresses, amorphous state) on the process being studied. In [26,27], it was shown that the amorphous state of aluminum leads to a lower degree of intensification of mutual diffusion than the amorphous state of titanium. However, with increasing temperature, devitrification of the amorphous phase of titanium can obviously occur and its effect on ignition will be minimal. At the same time, the presence of the Ti-Al interface can affect the devitrification temperature and increase the temperature range of existence of the amorphous phase. The above issue, in addition to the study of amorphous nanoparticles of titanium in a vacuum, is also considered in this work.

## Description of the model

To model the interatomic interactions within the Ti-Al system, EAM potentials from [28] were employed, which were derived through comparisons with experimental data and *ab initio* calculations for various properties and structures of metals Ti, Al, and intermetallics  $Ti_3Al$  and  $TiAl$ . These potentials have demonstrated their efficacy in various studies and have been successfully validated for a broad spectrum of mechanical and structural-energetic properties of Ti-Al alloys [26–31]. In particular, the potentials used by us show good agreement with experimental data on the melting temperature of Ti and Al: in molecular dynamics modeling, they turned out to be equal to 1995 and 990 K, respectively (reference values: 1943 and 933 K).

In the initial stage, a titanium particle was created by excising a sphere of the required size from an ideal crystal. The particle sizes considered ranged from 1.75 to 11 nm. For particles with a diameter below 1.75 nm, pinpointing the onset of crystallization proved challenging, while for particles with a diameter exceeding 11 nm, the impact of the free surface was already relatively small. Free space was simulated around the particle, that is, free boundary conditions and the NPT canonical ensemble were used. Temperature regulation was achieved using a Nose-Hoover thermostat. The time step for integration in the molecular dynamics method was set to 1 fs.

To simulate the aluminum layer around the titanium particle, a shell was created that contained approximately the same number of atoms as the particle. Initially, the shell was also cut out of an aluminum crystal. The thickness of the shell was sufficient, and further increasing it did not affect the results.

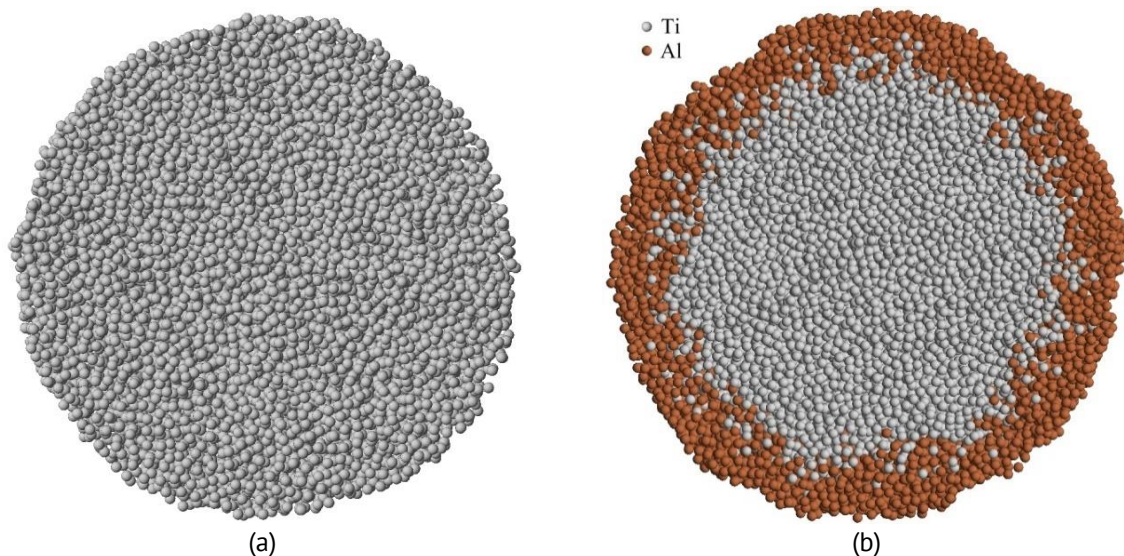


**Fig. 1.** Amorphous titanium nanoparticles with a diameter of 9 nm in vacuum (a) and in an aluminum shell (b). Particle cross-sections are shown

To produce the amorphous structure of the particles, ultra-fast cooling (with a cooling rate of approximately  $10^{16}$ – $10^{17}$  K/s) was implemented, following the melting of the particles via heating to 3000 K. At such a rapid cooling rate, homogeneous crystallization is unable to occur, resulting in the formation of an amorphous structure. The quality of the amorphous structure was assessed using radial distribution diagrams

of atoms and the average energy of atoms within the nanoparticle (with further details provided in the subsequent section). Furthermore, the destruction of the crystalline structure of the particles, as well as their crystallization, were typically discernible both visually and through the use of a crystalline phase visualizer. Examples of slices of amorphous titanium particles with a diameter of 9 nm in a vacuum and in an aluminum shell are shown in Fig. 1.

For particles of each size, heating was simulated at a constant rate of  $5 \cdot 10^{11}$  K/s. In similar tasks using molecular dynamics simulation, the rate of temperature change is usually set from  $10^{11}$  to  $10^{13}$  K/s [19–22]. In [20–22], it was shown that temperature change rates of  $5 \cdot 10^{12}$  K/s are already sufficient for homogeneous crystallization to occur. However, the lower the speed, the more accurately the temperature of the phase transition onset can be determined. On the other hand, the longer the computer experiment, the higher the mutual diffusion at the Ti-Al interface, which also affects the accuracy of determining the sintering temperature. According to our previous works [20,21], the speed in the range of  $5 \cdot 10^{11}$ – $10^{12}$  K/s turned out to be optimal in this case.

Simulation of devitrification was carried out with gradual heating from 700 to 1300 K for titanium particles without a shell and from 800 to 1400 K in the case of the presence of a shell. In both cases, the simulation duration was 1.2 ns.

## Results and Discussion

The average potential energy of titanium atoms was chosen as the main characteristic of the nanoparticle structure state. Figure 2 shows the dependencies of the average energy of titanium atoms on temperature for particles with diameters of 7 and 9 nm in vacuum and in an aluminum shell. Dotted lines also show the dependencies for a monocrystalline particle.

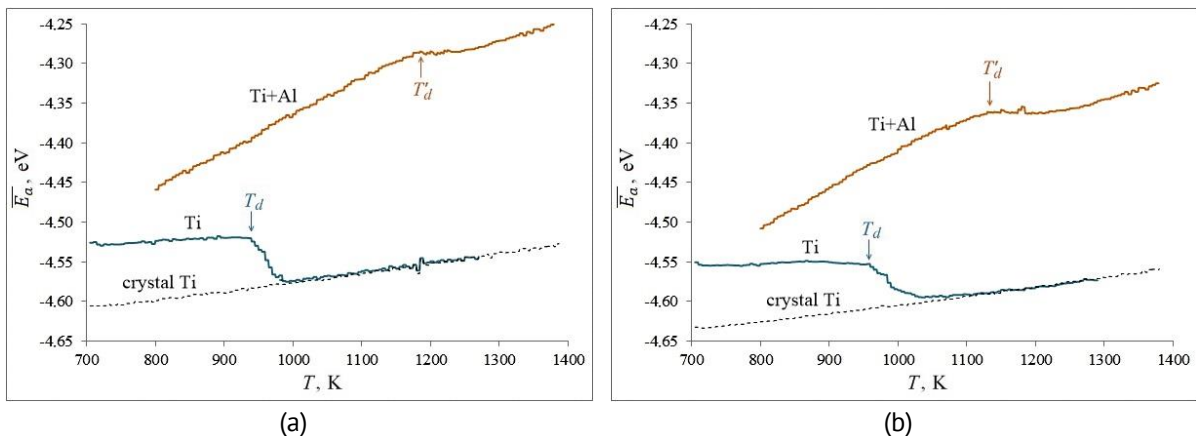


**Fig. 2.** Dependences of the average potential energy of Ti atoms on temperature during heating at a rate of  $5 \cdot 10^{11}$  K/s of an amorphous Ti particle in vacuum and in an aluminum shell: (a) with a diameter of 7 nm; (b) with a diameter of 9 nm. The dotted line shows the dependence for a single-crystal particle.  $T_d$  – devitrification temperature of an amorphous particle in vacuum,  $T'_d$  – in an aluminum shell

The sharp drops in the average energy of atoms on the graphs correspond to the phase transition – devitrification of amorphous particles during heating. As is known, phase transitions of melting-crystallization do not occur instantly, the crystal-liquid front

moves at a finite speed, which depends on temperature and usually amounts to several tens of meters per second [32,33]. In connection with this, the temperature of melting was determined by the moment of the onset of the phase transition (shown by arrows on the graph).

For particles in vacuum (lower graphs in Fig. 2), devitrification began at a temperature of approximately 940 K for a 7 nm diameter particle and 930 K for a 9 nm diameter particle. These values are higher than experimental ones: according to [34], for alloys with a high titanium content this temperature is about 700 – 800 K. However, it is known that in the molecular dynamics model a relatively long process of nucleation of crystallization centers is required and the beginning of this process is “delayed” at gradual change in temperature, and the higher the rate of temperature change, the higher the “delay” [20–22]. In addition, the potential used has some error in describing the devitrification process, which also affects the determination of the transition temperature.

After devitrification and crystallization of the entire particle in vacuum, the average energy of the atoms almost coincided with the energy of the single-crystalline particle. The considered rate of temperature increase was low enough to form a minimum density of defects during crystallization. If grain boundaries were formed, then, as a rule, they were low-energy – with a high density of coinciding nodes, often twins.

The graphs showing the change in average energy of titanium atoms for particles in an aluminum shell are located above in Fig. 2. This is because some titanium atoms diffused into the aluminum, and the potential energy of these atoms is higher than in the particle's bulk. The greater slope of the dependencies compared to those for particles in vacuum is also explained by diffusion. During the devitrification process of titanium particles in an aluminum shell, the decrease in the average energy of titanium atoms is significantly smaller compared to particles in vacuum, again due to the contribution of diffused titanium atoms in aluminum. After crystallization, the energy growth with increasing temperature became less intense, and the slopes of the dependencies decreased. This is explained by the reduction in the intensity of mutual diffusion in the crystalline state of titanium.

The presence of an aluminum shell, as shown in Fig. 2, significantly affects the devitrification temperature – it begins at a much higher temperature: approximately 1180 and 1130 K for particles with diameters of 7 and 9 nm, respectively.

To quantify the impact of the free surface of nanoparticles on their melting temperature, a mathematical formula is frequently employed, which assumes that the variation in the phase transition temperature is directly proportional to the ratio of the surface area to the volume of the particle. In the case of a spherical particle, this change should be proportional to  $N^{-1/3}$  or  $d^{-1}$ , where  $N$  represents the number of atoms in the particle, and  $d$  is its diameter. For the devitrification temperature, we adopted the same assumption, incorporating a correction  $\delta$  to account for the finite thickness of the surface layer of the particle or the diffusion zone in the case of an aluminum shell [20,21,31]:

$$T_d(d) = T_d^0 - \frac{A}{d-\delta} \quad (1)$$



Here  $T_d$  and  $T_d^0$  are the devitrification temperatures of the particle and bulk material;  $A$  is a parameter responsible for the degree of influence of the particle surface on its devitrification.

To construct approximation curves for the devitrification temperature of titanium nanoparticles in vacuum and in an aluminum shell, we utilized Eq. (1) and plotted them as dashed lines in Fig. 3. The markers in the figure represent the values derived from our model, which align quite well with the approximation curves. This agreement provides compelling evidence for the dominant influence of the interface, whether it be the free surface or the interphase boundary, in the devitrification process of nanoparticles. Values for Eq. (1) for titanium particles in vacuum:  $T_d^0 = 850$  K,  $A_d = -600$  K·nm,  $\delta = 0.4$  nm; in an aluminum shell:  $T_d^0 = 980$  K,  $A_d = -970$  K·nm,  $\delta = 1.4$  nm.

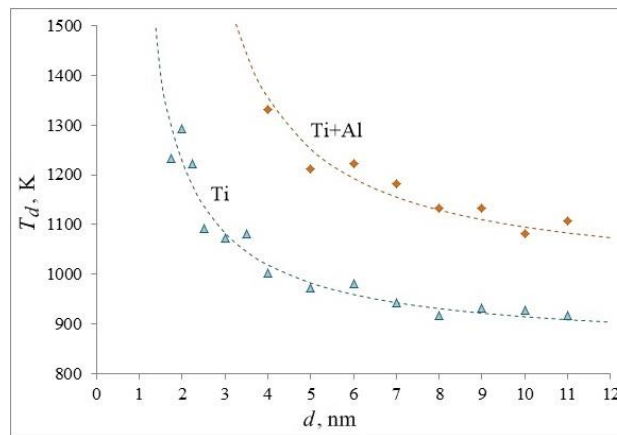


**Fig. 3.** The devitrification temperature of a titanium particle in a vacuum and in an aluminum shell depending on its diameter. Markers – model results, dotted lines – approximation

As can be seen, the influence of the aluminum shell on the devitrification temperature of titanium particles is quite significant – in the case of its presence, the devitrification temperature is approximately 200 K higher than for particles in vacuum. When considering the diffusion zone and the blurring of the particle boundary, the value of  $\delta$  increased by 1 nm, which roughly corresponds to the picture observed during modeling.

The value of  $A$  in Eq. (1) – the parameter responsible for the degree of influence of the particle boundary on the change in devitrification temperature compared to a massive sample – turned out to be negative. This means that if the melting temperature of nanoparticles decreases with a decrease in particle size, the devitrification temperature, on the contrary, increases. This can be explained as follows. The potential wells in which atoms are located on the surface or near defects are less deep and wider, blurred, due to less regular arrangement of neighboring atoms, thermal vibrations, and diffusion. Therefore, the presence of defects and interfaces reduces the probability of the nucleation of crystallization centers. However, on the other hand, the formation of these centers requires a certain mobility of atoms, that is, self-diffusion, which is more intense near the surface. This is well seen in Fig. 4, where the crystallization mechanism during devitrification was studied using a crystal phase visualizer. This visualizer determines the belonging of each atom to a certain crystalline structure based on the analysis of the

arrangement of neighboring atoms. In this case, a Ti atom was considered to belong to the hcp or fcc lattice if more than 75 % of its nearest neighbors (in this case, the number of nearest neighbors for atoms on the surface is approximately two times less than in the volume) were located close to the nodes of an ideal hcp or fcc crystal (accounting for thermal expansion) within a specified tolerance of 25 % from the radius of the first coordination sphere. Ti atoms that did not meet these conditions were considered to belong to an amorphous structure. It should be noted that the values of 75 and 25% were variable.

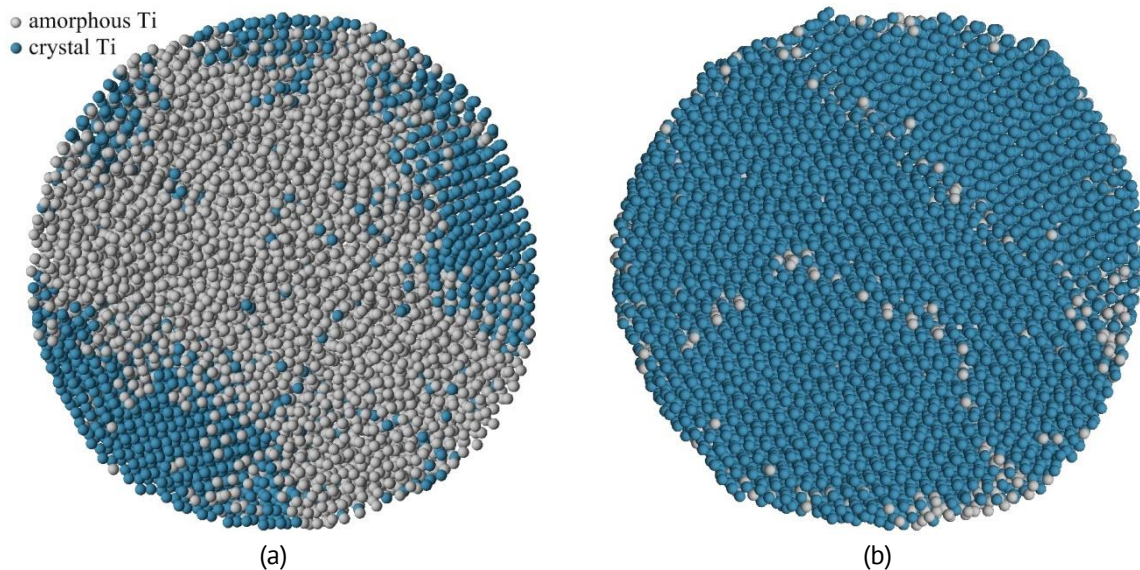


**Fig. 4.** Atomic structure of a slice of a titanium particle with a diameter of 9 nm at different moments of the devitrification process: (a) at the moment of formation of crystallization centers when the temperature reaches 890 K; (b) after the completion of crystallization. Green color highlights atoms with a nearest environment corresponding to a crystalline structure, gray – amorphous

As can be seen in Fig. 4, the formation of a crystalline structure occurs during devitrification from the surface, which is explained by a relatively larger contribution of self-diffusion near the surface in this case. After crystallization in the volume of the particle, as shown in the example, three grains were formed, separated by grain boundaries with relatively low energy (high density of coinciding nodes).

In the case of having an aluminum shell, the devitrification mechanism changed drastically (Fig. 5) – crystallization nuclei were formed not near the boundary but, typically, within the core of the titanium particle. Here, the factor of high mobility near the boundary disappears, and the formation of relatively deeper and narrower potential wells in the core of the particle takes precedence. Additionally, aluminum atoms, along with the presence of a diffusion zone, lead to the blurring of potential wells and a decrease in the likelihood of crystallization nuclei appearing near the interfacial boundary.

As for the aluminum shell, it was in an amorphous state throughout the entire heating simulation. When the starting bimetallic particles were created, it suddenly melted and cooled along with the Ti core (Fig. 1(b)). The devitrification of the Ti core upon subsequent heating occurred at a temperature above the melting point of aluminum.

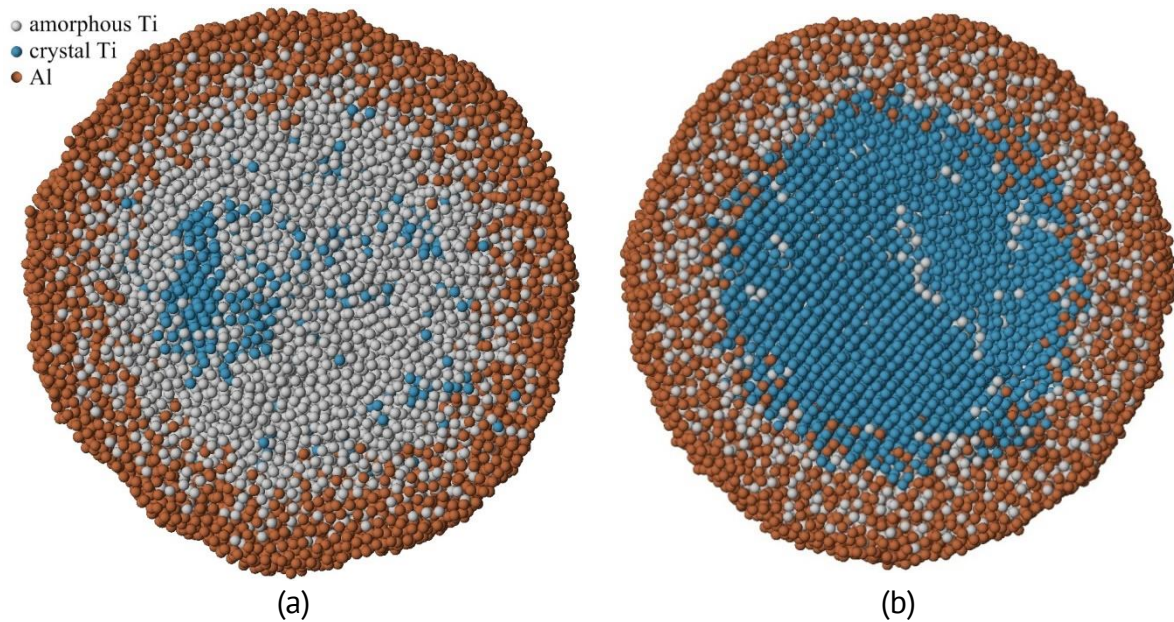


**Fig. 5.** Atomic structure of a slice of a titanium particle with a diameter of 9 nm in an aluminum shell at different moments of the devitrification process: (a) at the moment of formation of crystallization centers when the temperature reaches 1120 K; (b) after the completion of crystallization

The obtained result, i.e., the increase in the temperature range of the amorphous phase of metal nanoparticles in the shell of another metal, can likely be qualitatively extended to other binary systems. Moreover, a more significant influence of the shell on the increase in the devitrification temperature is probably expected with a greater difference in the radii of atoms of the two metals.

## Conclusions

The molecular dynamics method was used to study the devitrification process of titanium nanoparticles in vacuum and in an aluminum shell during heating at a rate of  $5 \cdot 10^{11}$  K/s. The investigation revealed that the devitrification temperature, in comparison to a massive sample, exhibits an inverse proportionality to the particle diameter, with a correction that accounts for the finite width of the surface layer or diffusion zone in the case of an aluminum shell. As the particle size diminishes, leading to an increased proportion of atoms in close proximity to the boundary, the devitrification temperature rises. The presence of an aluminum shell significantly increases the devitrification temperature of titanium nanoparticles – for the considered particle sizes, the difference was about 200 K. Thus, reducing the size of titanium particles and the presence of an aluminum shell increase the temperature range of the existence of the amorphous phase of titanium. The mechanisms of crystalline phase formation in particles in vacuum and in an aluminum shell differ significantly: in the first case, crystalline nuclei are formed near the surface, while in the second, on the contrary, in the volume of the particle.



## References

1. Schwarz JA, Lyshevski SE, Contescu CI. (eds.) *Dekker encyclopedia of nanoscience and nanotechnology*. Third ed. Boca Raton: CRC Press; 2014.
2. Liang S-X, Zhang LC, Reichenberger S, Barcikowski S. Design and perspective of amorphous metal nanoparticles from laser synthesis and processing. *Physical Chemistry Chemical Physics*. 2021;23: 11121–11154.
3. Sun J, Sinha SK, Khammari A, Picher M, Terrones M, Banhart F. The amorphization of metal nanoparticles in graphitic shells under laser pulses. *Carbon*. 2020;161: 495–501.
4. He DS, Huang Y, Myers BD, Isheim D, Fan X, Xia G-J, Deng Y, Xie L, Han S, Qiu Y, Wang Y-G, Luan J, Jiao Z, Huang L, Dravid VP, He J. Single-element amorphous palladium nanoparticles formed via phase separation. *Nano Research*. 2022;15: 5575–5580.
5. Qian Y, Silva A, Yu E, Anderson CL, Liu Y, Theis W, Ercius P, Xu T. Crystallization of nanoparticles induced by precipitation of trace polymeric additives. *Nature Communications*. 2021;12: 2767.
6. Pei Y, Zhou G, Luan N, Zong B, Qiao M, Tao F. Synthesis and catalysis of chemically reduced metal-metalloid amorphous alloys. *Chemical Society Reviews*. 2012;41: 8140–8162.
7. Jia Z, Wang Q, Sun L, Wang Q, Zhang LC, Wu G, Luan JH, Jiao ZB, Wang A, Liang SX, Gu M, Lu J. Metallic glass catalysts: attractive in situ self-reconstructed hierarchical gradient structure of metallic glass for high efficiency and remarkable stability in catalytic performance. *Advanced Functional Materials*. 2019;29: 1807857.
8. Chen Q, Yan Z, Guo L, Zhang H, Zhang L-C, Wang W. Role of maze like structure and  $Y_2O_3$  on Al-based amorphous ribbon surface in MO solution degradation. *Journal of Molecular Liquids*. 2020;318: 114318.
9. Yang BJ, Yao JH, Zhang J, Yang HW, Wang JQ, Ma E. Al-rich bulk metallic glasses with plasticity and ultrahigh specific strength. *Scripta Materialia*. 2009;61: 423–426.
10. Schroers J, Johnson WL. Ductile bulk metallic glass. *Physical Review Letters*. 2004;93: 255506.
11. Wagener P, Jakobi J, Rehbock C, Chakravadhanula VSK, Thede C, Wiedwald U, Bartsch M, Kienleand L, Barcikowski S. Solvent-surface interactions control the phase structure in laser-generated iron-gold core-shell nanoparticles. *Scientific Reports*. 2016;6: 23352.
12. Ziefub AR, Reichenberger S, Rehbock C, Chakraborty I, Gharib M, Parak WJ, Barcikowski S. Laser fragmentation of colloidal gold nanoparticles with high-intensity nanosecond pulses is driven by a single-step fragmentation mechanism with a defined educt particle-size threshold. *The Journal of Physical Chemistry C*. 2018;122: 22125–22136.
13. Amikura K, Kimura T, Hamada M, Yokoyama N, Miyazaki J, Yamada Y. Copper oxide particles produced by laser ablation in water. *Applied Surface Science*. 2008;254: 6976–6982.
14. Barcikowski S, Compagnini G. Advanced nanoparticle generation and excitation by lasers in liquids. *Physical Chemistry Chemical Physics*. 2013;15: 3022–3026.
15. Buffat P, Borel J-P. Size effect on the melting temperature of gold particles. *Physical Review A*. 1976;13: 2287.
16. Allen GL, Bayles RA, Gile WW, Jesser WA. Small particle melting of pure metals. *Thin Solid Films*. 1986;144: 297–308.
17. Castro T, Reifenberger R, Choi E, Andres RP. Size-dependent melting temperature of individual nanometer-sized metallic clusters. *Physical Review B*. 1990;42: 8548.
18. Chepkasov IV, Gafner YY, Vysotin MA, Redel LV. A study of melting of various types of Pt-Pd nanoparticles. *Physics of the Solid State*. 2017;59: 2076–2081.
19. Qi Y, Cagin T, Johnson WL, Goddard III WA. Melting and crystallization in Ni nanoclusters: the mesoscale regime. *The Journal of Chemical Physics*. 2001;115: 385–394.
20. Poletaev GM, Bebikhov YV, Semenov AS. Molecular dynamics study of the formation of the nanocrystalline structure in nickel nanoparticles during rapid cooling from the melt. *Materials Chemistry and Physics*. 2023;309: 128358.
21. Poletaev GM, Gafner YY, Gafner SL. Molecular dynamics study of melting, crystallization and devitrification of nickel nanoparticles. *Letters on Materials*. 2023;13(4): 298–303.
22. Nguyen TD, Nguyen CC, Tran VH. Molecular dynamics study of microscopic structures, phase transitions and dynamic crystallization in Ni nanoparticles. *RSC Advances*. 2017;7: 25406–25413.
23. Boldyrev VV, Tkacova K. Mechanochemistry of solids: past, present, and prospects. *Journal of Materials Synthesis and Processing*. 2000;8: 121–132.
24. Filimonov VY, Loginova MV, Ivanov SG, Sitnikov AA, Yakovlev VI, Sobachkin AV, Negodyaev AZ, Myasnikov AY. Peculiarities of phase formation processes in activated Ti+Al powder mixture during

- transition from combustion synthesis to high-temperature annealing. *Combustion Science and Technology*. 2020;192: 457–470.
25. Loginova MV, Yakovlev VI, Filimonov VY, Sitnikov AA, Sobachkin AV, Ivanov SG, Gradoboev AV. Formation of structural states in mechanically activated powder mixtures Ti+Al exposed to gamma irradiation. *Letters on Materials*. 2018;8: 129–134.
26. Poletaev GM, Bebikhov YV, Semenov AS, Sitnikov AA. Molecular dynamics investigation of the effect of the interface orientation on the intensity of titanium dissolution in crystalline and amorphous aluminum. *Journal of Experimental and Theoretical Physics*. 2023;136(4): 477–483.
27. Poletaev GM, Bebikhov YV, Semenov AS, Sitnikov AA, Yakovlev VI. Molecular dynamics study of the dissolution of titanium nanoparticles in aluminum. *Materials Physics and Mechanics*. 2023;51(5): 9–15.
28. Zope RR, Mishin Y. Interatomic potentials for atomistic simulations of the Ti-Al system. *Physical Review B*. 2003;68: 024102.
29. Kim Y-K, Kim H-K, Jung W-S, Lee B-J. Atomistic modeling of the Ti-Al binary system. *Computational Materials Science*. 2016;119: 1–8.
30. Pei Q-X, Jhon MH, Quek SS, Wu Z. A systematic study of interatomic potentials for mechanical behaviours of Ti-Al alloys. *Computational Materials Science*. 2021;188: 110239.
31. Poletaev G, Gafner Y, Gafner S, Bebikhov Y, Semenov A. Molecular dynamics study of the devitrification of amorphous copper nanoparticles in vacuum and in a silver shell. *Metals*. 2023;13(10): 1664.
32. Chan W-L, Averback RS, Cahill DG, Ashkenazy Y. Solidification velocities in deeply undercooled silver. *Physical Review Letters*. 2009;102: 095701.
33. Zhang HY, Liu F, Yang Y, Sun DY. The molecular dynamics study of vacancy formation during solidification of pure metals. *Scientific Reports*. 2017;7: 10241.
34. Susic MV. Kinetics of devitrification (crystallization) of amorphous titanium. *Materials Chemistry and Physics*. 1985;12: 99–109.

## About Authors

### Gennady M. Poletaev

*Doctor of Physical and Mathematical Sciences*

*Leading Researcher (Khakass State University, Abakan, Russia)*

*Head of Department (Polzunov Altai State Technical University, Barnaul, Russia)*

### Yuri Ya. Gafner

*Doctor of Physical and Mathematical Sciences*

*Head of Department (Khakass State University, Abakan, Russia)*

### Svetlana L. Gafner

*Doctor of Physical and Mathematical Sciences*

*Professor (Khakass State University, Abakan, Russia)*

### Irina V. Zorya

*Doctor of Physical and Mathematical Sciences*

*Head of Department (Siberian State Industrial University, Novokuznetsk, Russia)*

### Yuriy V. Bebikhov

*Candidate of Physical and Mathematical Sciences*

*Assistant Professor (Polytechnic Institute of North-Eastern Federal University, Mirny, Russia)*

### Alexander S. Semenov

*Doctor of Physical and Mathematical Sciences*

*Director of the Institute (Polytechnic Institute of North-Eastern Federal University, Mirny, Russia)*